




Decyl Gallate as a Possible Inhibitor of N-Glycosylation Process in *Paracoccidioides lutzii*

 Ana Carolina Alves de Paula e Silva,^a Haroldo Cesar de Oliveira,^a Liliana Scorzoni,^a Caroline Maria Marcos,^a Claudia Tavares dos Santos,^a Ana Marisa Fusco-Almeida,^a Ana Carolina Guerta Salina,^{b,c} Alexandra Ivo Medeiros,^b Fausto Almeida,^d Sheena Claire Li,^{e,f} Charles Boone,^e Maria J. S. Mendes-Giannini^a

^aDepartment of Clinical Analysis, Faculdade de Ciências Farmacêuticas, Universidade Estadual Paulista, Araraquara, São Paulo, Brazil

^bDepartment of Biological Sciences, Faculdade de Ciências Farmacêuticas, Universidade Estadual Paulista, Araraquara, São Paulo, Brazil

^cDepartment of Biochemistry and Immunology, Faculdade de Medicina de Ribeirão Preto, Universidade de São Paulo, Ribeirão Preto, São Paulo, Brazil

^dDepartment of Cellular/Molecular Biology and Pathogenic Bioagents, Faculdade de Medicina de Ribeirão Preto, Universidade de São Paulo, Ribeirão Preto, São Paulo, Brazil

^eDepartment of Molecular Genetics, Terrence Donnelly Centre for Cellular and Biomolecular Research, University of Toronto, Toronto, Ontario, Canada

^fRIKEN Center for Sustainable Resource Science, Saitama, Japan

ABSTRACT The available antifungal therapeutic arsenal is limited. The search for alternative drugs with fewer side effects and new targets remains a major challenge. Decyl gallate (G14) is a derivative of gallic acid with a range of biological activities and broad-spectrum antifungal activity. Previously, our group demonstrated the promising anti-*Paracoccidioides* activity of G14. In this work, to evaluate the antifungal characteristics of G14 for *Paracoccidioides lutzii*, a chemical-genetic interaction analysis was conducted on a *Saccharomyces cerevisiae* model. N-glycosylation and/or the unfolded protein response pathway was identified as a high-confidence process for drug target prediction. The overactivation of unfolded protein response (UPR) signaling was confirmed using this model with IRE1/ATF6/PERK genes tagged with green fluorescent protein (GFP). In *P. lutzii*, this prediction was confirmed by the low activity of glycosylated enzymes [α -(1,3)-glucanase, *N*-acetyl- β -D-glucosaminidase (NAGase), and α -(1,4)-amylase], by hyperexpression of genes involved with the UPR and glycosylated enzymes, and by the reduction in the amounts of glycosylated proteins and chitin. All of these components are involved in fungal cell wall integrity and are dependent on the N-glycosylation process. This loss of integrity was confirmed by the reduction in mitochondrial activity, impaired budding, enhancement of wall permeability, and a decrease in viability. These events led to a reduction of the ability of fungi to adhere on human lung epithelial cells (A549) *in vitro*. Therefore, G14 may have an important role in balancing the inflammatory reaction caused by fungal infection, without interfering with the microbicidal activity of nitric oxide. This work provides new information on the activity of G14, a potential anti-*Paracoccidioides* compound.

KEYWORDS *Paracoccidioides lutzii*, decyl gallate, chemical-genetic interaction, N-glycosylation, mechanisms of action

Paracoccidioidomycosis (PCM) is a systemic infection caused by the species complex *Paracoccidioides* spp., including *Paracoccidioides lutzii*. This disease occurs in areas with poor socioeconomic conditions, located mainly in Latin America and in active rural areas in Brazil. Despite the availability of antifungal agents for the treatment of PCM, the selection of the therapy depends on the severity of the disease and the type of antifungal agent available (amphotericin B, azoles, and sulfonamides) (1). In addition, this therapy requires a long treatment period, has many cases of relapse, and frequently comes with side effects and high toxicity, resulting in low quality of life for the patient

Citation de Paula e Silva ACA, de Oliveira HC, Scorzoni L, Marcos CM, Santos CTD, Fusco-Almeida AM, Salina ACG, Medeiros AI, Almeida F, Li SC, Boone C, Mendes-Giannini MJS. 2019. Decyl gallate as a possible inhibitor of N-glycosylation process in *Paracoccidioides lutzii*. *Antimicrob Agents Chemother* 63:e01909-18. <https://doi.org/10.1128/AAC.01909-18>.

Copyright © 2019 American Society for Microbiology. All Rights Reserved.

Address correspondence to Ana Carolina Alves de Paula e Silva, ana_alpasi@hotmail.com, or Maria J. S. Mendes-Giannini, gianninimj@gmail.com.

Received 6 September 2018

Returned for modification 30 March 2019

Accepted 28 July 2019

Accepted manuscript posted online 26 August 2019

Published 22 October 2019

TABLE 1 Top 10 deletion mutants sensitive to G14

Mutant	z-score	Name and/or description
VPS13	−10.1938	Vacuolar protein sorting
IRE1	−14.2456	Inositol requiring
HAC1	−15.172	Homologous to Atf/Creb1
UBR2	−8.99919	Cytoplasmic ubiquitin-protein ligase
CTF3	−9.53256	Chromosome transmission fidelity
HST3	−9.29459	Homolog of SIR2
CTI6	−8.44196	Cyc8-Tup1-interacting protein
PEX14	−7.77147	Peroxisome related
YHR003C	−9.02499	tRNA threonyl-carbamoyl-adenosine dehydratase
YKR041W	−8.24314	

(2). Therefore, none of the currently available therapies ensures the complete elimination of the fungus from the patient (1).

The investment in the development of new antifungal agents with higher efficacy and fewer side effects is of extreme importance in order to increase the treatment options for this disease. However, this development is a challenge since the pathogenic fungi and their host share the same characteristics of eukaryotic cells.

In this respect, the demand for new antifungal compounds, especially those obtained from natural origin or their synthetic derivatives, is of extreme importance, and PCM experts have been working to find new agents from natural sources (3–9).

Chemical studies of ethanolic extract obtained from the leaves of *Alchornea glandulosa* identified the presence of phenolic compounds, such as gallic acid, which has a range of biological activities, including anti-inflammatory and antifungal activity (10–13). Structurally, modifications were made in this molecule by the addition of variably sized carbon chains, resulting in the formation of alkyl gallates. They have been described as having great antifungal activity against a representative panel of opportunistic pathogenic fungi (14).

Our group demonstrated that decyl gallate (G14) had great antifungal activity *in vitro* against 18 pathogenic fungi species (including eight different *Paracoccidioides* isolates). For *Paracoccidioides* isolates, G14 presented a low MIC and a good selectivity index value (>10) against infection in human lung epithelial cells (A549) and normal fibroblast pulmonary cells (MRC-5) (8). These results showed that G14 is an excellent candidate for a broad-spectrum antifungal prototype and encouraged us to try to discover its mechanism of action.

Therefore, our study using a chemical-genetic interaction assay (15–19) provided comprehensive information about the effect of specific gene perturbations on the cell's response to G14 treatment, which, in addition to other assays, had demonstrated that G14 has a strong influence on the N-glycosylation process, highlighting G14 as a potential anti-*Paracoccidioides* agent.

RESULTS

N-glycosylation/UPR as a target of G14 treatment. To elucidate the G14 mode of action and cellular target, a chemical-genetic interaction analysis was conducted. A *Saccharomyces cerevisiae* gene deletion mutant pool was treated with G14 and different controls. The relative fitness of each yeast mutant was quantified by sequencing strain-specific DNA barcodes treated with G14 and comparing fitness levels to that of the dimethyl sulfoxide (DMSO) control. The top 10 deletion mutants susceptible to G14 (Table 1) were subjected to enrichment analysis, and enrichment was found for genes involved in the gene ontology (GO) category cellular/endoplasmic reticulum (ER) unfolded protein response (UPR) ($P < 0.01$). The deletion mutants of HAC1 and IRE1 were the most hypersensitive to G14. This profile was similar to the chemical-genetic interaction profile of the control agent tunicamycin, which inhibits the N-glycosylation pathway. The Pearson correlation coefficient between G14 and tunicamycin profiles was calculated (0.1906) and showed a moderate level of profile similarity between the two compounds (Fig. 1). Assuming that the chemical inhibitor of a gene product tends

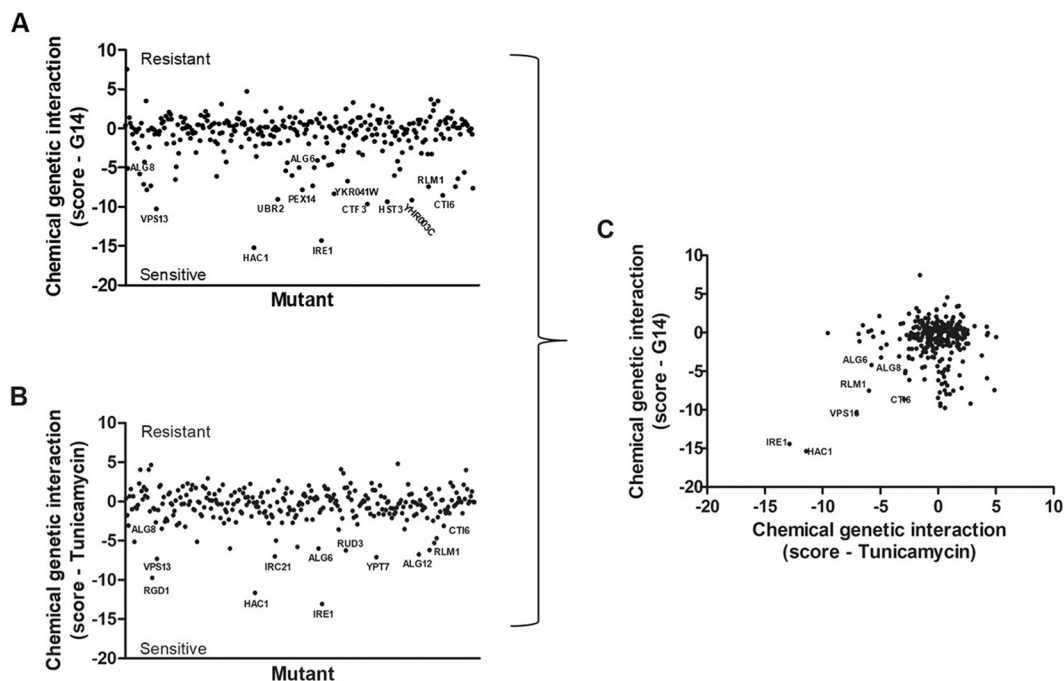


FIG 1 G14 and tunicamycin had similar profiles. The chemical genetic interaction score (y axis) of each mutant (x axis) was plotted for G14 (A) and tunicamycin (B), highlighting the hypersensitive mutants. The profile similarity was demonstrated by the Pearson correlation coefficient (0.1906) (C).

to mimic the loss-of-function phenotype of a mutant that inactivates the gene, the chemical-genetic interaction profile for a bioactive compound can resemble the genetic interaction profile for the target. The comparison of the chemical-genetic interaction profile of G14 with the genetic interaction network of *S. cerevisiae* allowed us to predict the target for the compound as ALG12, which has a genetic interaction profile most significantly correlated to the chemical-genetic interaction profile of G14. ALG12 is a nonessential gene responsible for the addition of alpha-1,6-mannose to dolichol-linked proteins, acting in the dolichol pathway for N-glycosylation.

UPR hyperactivation after G14 challenge. The gene IRE1 is a mediator of the yeast unfolded protein response (UPR) and coordinates a series of responses by a signal transduction pathway that maintains endoplasmic reticulum homeostasis. Activation of IRE1 is closely linked to the activation of HAC1. Both are essential for the proper functioning of this response (20). The susceptibility to G14 of mutants of IRE1 and HAC1 means that this pathway was essential to yeast survival after G14 exposure. For this reason, a UPR activation assay was performed against G14 in *S. cerevisiae* yeast strains containing green fluorescent protein (GFP) tags on the IRE1, ATF6, and PERK genes. We investigated if this pathway would be activated after treatment. By fluorescence microscopy observation (Fig. 2A) and with the analysis of the mean fluorescence intensity (MFI) (Fig. 2B), an increase in fluorescence intensity of the cells was verified after 3 h of G14 treatment, and this phenotype persisted after 24 h. Under normal conditions, this pathway has low activity, similar to that of the control DMSO at a nontoxic concentration; however, upon G14 treatment, this pathway was activated, and the transcription products containing the GFP sequence increased. The hyperactivation of the UPR upon treatment revealed that G14 led to stress in the endoplasmic reticulum and affected the correct protein folding.

G14 treatment changed N-glycosylated proteins profile of *P. lutzii*. Since the mechanism of action of G14 was linked to the N-glycosylation pathway and/or the response of unfolded proteins, the analysis of important enzymes belonging to remodeling and maintenance of the fungal cell wall was indicated. This is based on the idea that these enzymes are dependent on the N-glycosylation process in order to be

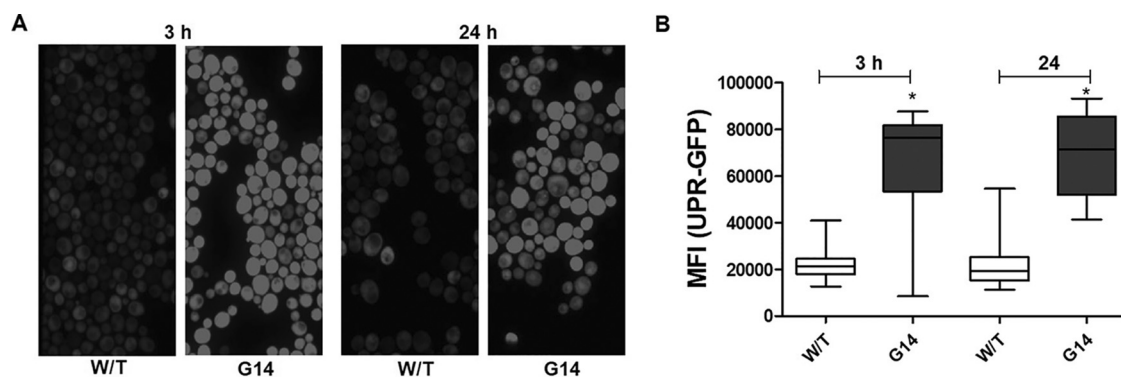


FIG 2 G14 treatment led to UPR hyperactivity. An *S. cerevisiae* yeast strain with GFP tags on genes belonging to the unfolded protein response (genes IRE1, ATF6, and PERK) was treated with decyl gallate (G14) for 3 and 24 h. (A) GFP-tagged protein expression was observed by fluorescence microscopy. (B) The mean fluorescence intensity (MFI) was measured. Control (W/T), without treatment. *, $P < 0.05$.

functional. Supporting this idea, the relative activities of the enzymes α -(1,3)-glucanase, *N*-acetyl- β -D-glucosaminidase, and α -(1,4)-amylase, after treatment with 0.5 μ g/ml of G14 were reduced by almost 50% compared to level of the control without treatment (Fig. 3A).

The N-glycosylation process occurs at the posttranslational level and is an essential process for the functioning of these enzymes; we thus tested if the decrease in the activity of the final protein (enzyme) was affected by the decreased expression of the involved genes (Table 2). After treatment with G14, it was observed that all the

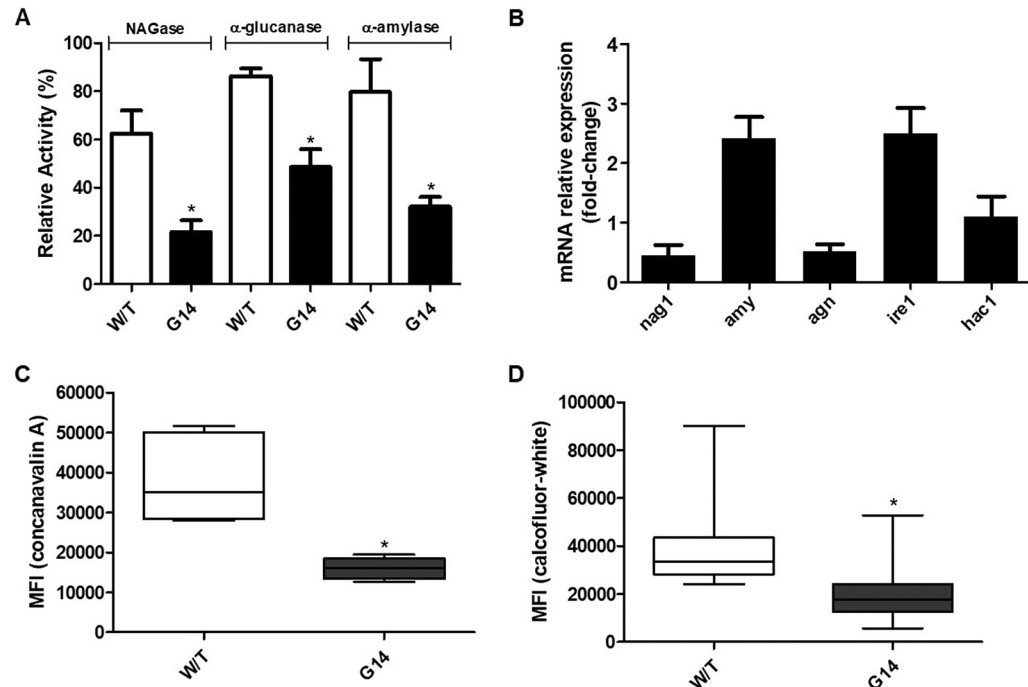


FIG 3 G14 changed the normal profiles of N-glycosylated proteins of *P. lutzii*. The fungal cells were treated with decyl gallate (G14) for 72 h. (A) Percentage of relative activity of the N-glycosylated enzymes was determined for the following: *N*-acetyl- β -D-glucosaminidase (NAGase), α -(1,3)-glucanase, and α -(1,4)-amylase (α -amylase). Control (W/T), without treatment. (B) Real-time PCR analysis of relative expression was conducted for the genes encoding *N*-acetyl- β -D-glucosaminidase (*nag1*), α -(1,4)-amylase (*amy*), α -(1,3)-glucanase (*agn*), and the endoplasmic reticulum stress-sensing genes inositol requiring enzyme-1 (*ire1*) and transcription factor (*hac1*). (C) Glycosylated proteins present in fungal wall were labeled with Alexa Fluor 488-conjugated concanavalin A, and the mean fluorescence intensity (MFI) was evaluated by flow cytometry. (D) Chitin amount was quantified using calcofluor white label and fluorescence microscopy. Control (W/T), without treatment. *, $P < 0.05$.

TABLE 2 Specific primers for coding genes

Primer name ^a	Sequence
nag1_F	TCATGCAGAGCTGGAACAAC
nag1_R	CATTGTAGCGGTGGTCATTG
agn_F	CAACCATGGTCAGCAAACAC
agn_R	CTGTAGCCCTGAACCCACAT
amy_F	CGGTGACTTGTATGGCCTTT
amy_R	CAGTTGGCCATTACATGACG
ire1_F	CCCCAGAGATATCGTGAGA
ire1_R	TTAGAACGTGGGGCCTAATG
hac1_F	CTTGCCCCATCCTCTTCAA
hac1_R	TTCAAGGATCCCTCCAACCTG
tub_F	CTGTTACCAGCCTCCCATATA
tub_R	TGCTTCAGAAATGGCAGTTG

^aF, forward; R, reverse.

analyzed genes (*agn*, *nag1*, *amy*, *ire1*, and *hac1*) showed an increase in expression (Fig. 3B) compared to the level of gene expression of the sample without treatment.

It was possible to observe that the G14 treatment reduced the amount of glycosylated proteins present in the fungal cell wall. The MFI of concanavalin A (ConA) (Fig. 3C), which is a lectin able to bind to glycosylated proteins, decreased 58% upon treatment, and calcofluor white (CFW) (Fig. 3D), which binds specifically with chitin, which is present in the cell wall and dependent on N-glycosylated-enzymes, decreased 50%.

G14 impaired *P. lutzii* development and viability. An MTT (3-[4,5-dimethylthiazol-2-yl]-2,5-diphenyl tetrazolium bromide) assay showed that G14 treatment led to 42% and 65% reductions in mitochondrial activity after 24 h and 48 h of treatment, respectively, compared to the levels of the control without treatment (Fig. 4A). The treatment damaged the development of *P. lutzii* cells since the treated cells showed a budding percentage of 50% at both times, indicating a decrease in new bud formation, while the control without treatment presented budding in about 90% of fungal cells (Fig. 4B). By trypan blue assay, we observed reductions of 39% and 53% in the rate of fungal cells excluding the blue dye after 24 and 48 h of G14 treatment, respectively (Fig. 4C). In the CFU analysis, reduction of 62% and 85% in growth, respectively, were observed after treatment with G14 (Fig. 4D). Together, these data demonstrated that G14 treatment impaired the maintenance of the fungal wall, reducing the cellular viability of the fungus.

G14 treatment reduced adhesion of *P. lutzii*. Although we observed a tendency toward a reduction of the internalization of *P. lutzii* in A549 cells after G14 treatment, this reduction was not significant compared to levels in the control without treatment. On the other hand, adhesion, an essential step in *Paracoccidioides* sp. infection, decreased 75% after G14 treatment (Fig. 5A). In order to know if the treatment affected the internalized fungal cells, CFU enumeration was performed. The results showed that there was not a reduction in CFU counts compared to level of the control without treatment (Fig. 5B). Even though the G14 treatment had not reached the internalized fungi in A549 cells, G14 showed important activity on a fungal virulence factor, adhesion.

G14 improved the antifungal activity of macrophages. When macrophages were treated only with G14, we observed a reduction of 62% in the nitrite concentration compared to that in macrophages stimulated with lipopolysaccharide (LPS). The same was observed during the infection of macrophages by *P. lutzii*. When the infection was treated with G14, we observed a reduction of 55% in the nitrite concentration compared to the level in the control without treatment (Fig. 6A). These results showed the anti-inflammatory activity of G14. We observed a reduction in CFU numbers when the infection was treated with G14 (Fig. 6B), suggesting that G14 contributed to macrophage activity against *P. lutzii*.

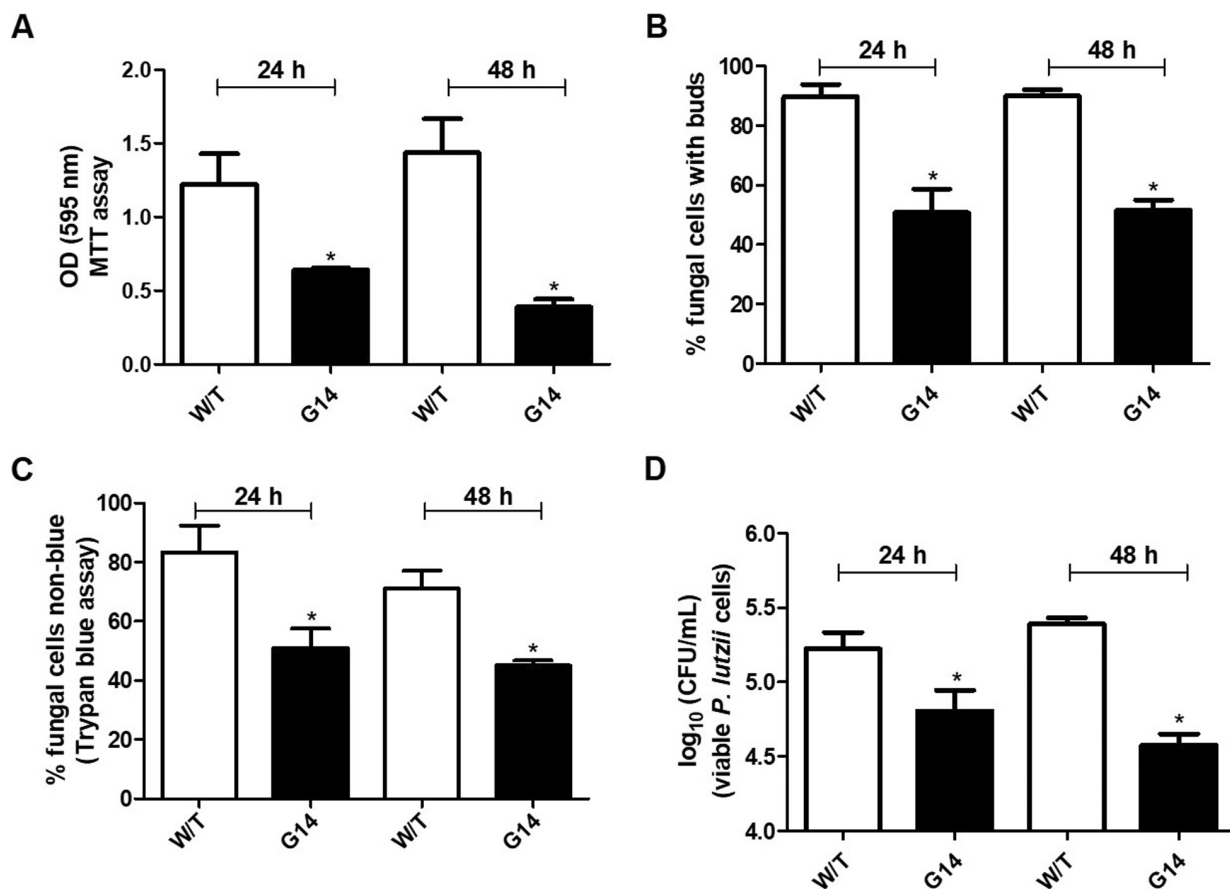


FIG 4 The development of *P. lutzii* cells was reduced after G14 treatment. Comparative analysis between the untreated control (W/T, without treatment) and of *P. lutzii* cells treated with decyl gallate (G14) after 24 h and 48 h. (A) MTT assay for mitochondrial activity of *P. lutzii* cells. OD, optical density. (B) Development assay with analysis of percentage of *P. lutzii* cells with buds. (C) Trypan blue assay for analysis of fungal wall permeability. (D) CFU assay to analyze the recovery of viable fungal cells. *, $P < 0.05$.

DISCUSSION

In order to know the mechanism of action of G14 in *Paracoccidioides* spp., we used a chemical-genetic interaction assay using *S. cerevisiae* as a model to predict the mechanism of action of G14 (decyl gallate). In the chemical-genetic interaction, a sublethal concentration of a growth-inhibitory compound was screened, and the

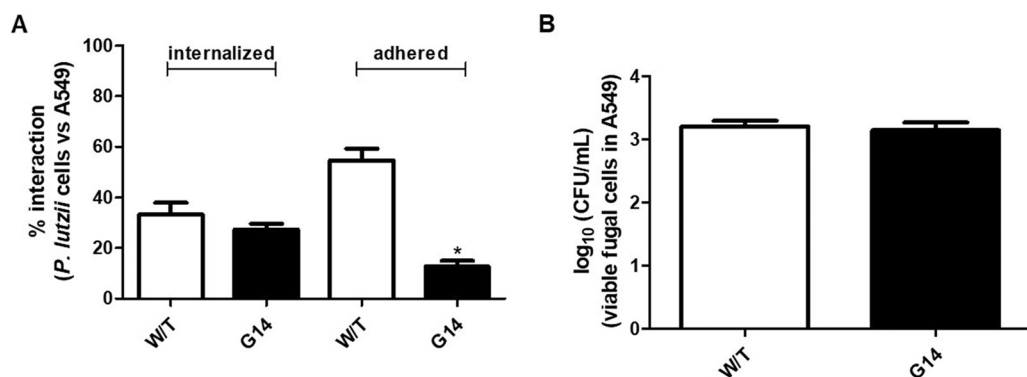


FIG 5 *In vitro* G14 decreased adhesion rate of *P. lutzii* in human pneumocytes. After 6 h of *P. lutzii* infection in A549 cells (human pneumocyte type I line), treatment with decyl gallate (G14) was performed for 24 h. (A) A quenching assay was performed to obtain the rate of adhesion and internalization by flow cytometry analysis. (B) The viability of internalized fungal cells was assessed by CFU counts in BHI agar plates. Control (W/T), without treatment. *, $P < 0.05$.

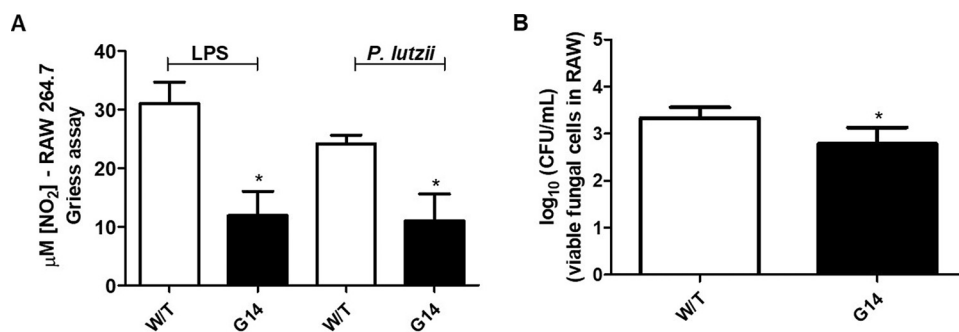


FIG 6 G14 decreased nitrite production by macrophages infected *in vitro* with *P. lutzii*. A RAW 264.7 macrophage monolayer was stimulated with LPS (positive control) and infected with *P. lutzii* for 6 h and subsequently treated with decyl gallate (G14) for 24 h. (A) Griess assay was performed to verify the ability of G14 to modulate nitrite production. (B) The infection was plated on BHI agar plates, and CFU counts were determined. Control (W/T), without treatment. *, $P < 0.05$.

deletion mutants with hypersensitive profiles were highlighted. The next step was the comparison of a chemical-genetic interaction profile to a compendium of genetic interactions (synthetic lethal). A synthetic lethal genetic interaction is characterized by the deletion of a single gene, resulting in viable mutants. However, a lethal phenotype is observed when double deletions are combined in the same mutant strain. Gene deletion alleles that show chemical-genetic interactions with a compound should also be synthetically lethal or synthetically sick as a result of a mutation in the compound target gene. Genetic profile similarities are measured for all gene pairs by computing Pearson correlation coefficients (PCC) from the complete genetic interaction matrix. These profiles predict the pathways and targets inhibited by treatment (15–19).

Based on the chemical-genetic interaction profile, we predicted that G14 affects the N-glycosylation and protein folding pathways. The profile was similar to that of one of our control compounds, tunicamycin. This compound is classified as a nucleoside antibiotic and inhibits N-glycosylation by blocking the first step in the synthesis of the dolichol-linked oligosaccharide, the transfer of UDP-*N*-acetylglucosamine to dolichol phosphate (21).

This result was confirmed when the chemical-genetic interaction profile of G14 was compared to the genetic interaction network of *S. cerevisiae*, allowing the prediction of its putative molecular target, alpha-1,6-mannosyltransferase (ALG12). ALG12 is localized in the endoplasmic reticulum (ER) and is responsible for the addition of alpha-1,6-mannose to dolichol-linked Man7GlcNAc2 and acts in the dolichol pathway for N-glycosylation (22).

N-glycosylation is an essential process for posttranslational modification of proteins. Some proteins are synthesized in the ribosomal portion of the rough endoplasmic reticulum (RER), where they assume their correct conformation. After this, there is an addition of a precursor oligosaccharide by transferase. The process of linking the protein with the oligosaccharide is called N-glycosylation (23).

It is known that N-glycosylation is an important process for fungal cells. The fungal cell wall is composed of polysaccharides, such as glucans, chitin, lipids, and proteins, some of which are highly glycosylated (glycoproteins). Since the fungal cell wall is essential for osmotic homeostasis maintenance, morphogenesis, and maintenance of the cellular form and for a role in mechanical resistance, it is considered a promising target for the development of new agents (24). In *Paracoccidioides* this role is not different; N-glycosylated proteins are crucial for many biological processes (25).

G14 affected the same pathway affected by tunicamycin, which had an effect on wall composition and development of *Paracoccidioides* spp. A study by Dos Reis Almeida et al. (26) showed that upon tunicamycin treatment, the level of N-glycosylation was lower, and a reduction of α -(1,4)-amylase activity, a glycosylated enzyme, was observed.

Thinking about glycosylated proteins, analysis of the relative activity of essential glycosylated enzymes present in the cell wall of *P. lutzii*, such as α -(1,3)-glucanase, *N*-acetyl- β -D-glucosaminidase, and α -(1,4)-amylase, after G14 treatment was proposed. These enzymes are responsible for covalently joining components to form a three-dimensional matrix of chitins, glucans, and glycoproteins. It is known that the loss of any of these components may impair the growth, morphology, and viability of the fungal cell (24). Our results showed that G14 treatment of *P. lutzii* reduced the relative activity of these enzymes, suggesting that G14 impairs the N-glycosylation process. Interestingly, the analysis of the expression of genes encoding these enzymes showed upregulation of these genes upon G14 treatment. We believe that this could possibly be a compensatory mechanism for diminished enzymatic activity due to the lack of N-glycosylation (27).

In order to demonstrate the extent of the treatment effect on the N-glycosylation pathway, we used the markers concanavalin A, which has a high affinity for glycosylated structures (28), and calcofluor white, which binds to chitin, a cell wall component dependent on the glycosylated enzymes that we tested in this study (28). The fluorescence of both markers upon treatment with G14 was lower than that in fungal cells without treatment. This reduction suggests that glycosylated enzymes as well chitin amounts are decreased after G14 treatment, probably due to its action in damaging the N-glycosylation process of these components.

When the N-glycosylation process is compromised, unfolded proteins are formed. The consequence is the generation of toxic signals to cells, leading to a stress situation. In eukaryotes, the endoplasmic reticulum stress response is orchestrated by at least three genes: IRE1, ATF6, and PERK. Together, these sensors coordinate the unfolded protein response (UPR), which is responsible for circumventing this situation and restoring homeostasis. In fungi, neither ATF6 nor PERK has been described, but IRE1 is considered the main mediator of homeostasis in response to unfolded proteins. The activation of IRE1 is closely linked to the activation of HAC1, and both are essential for the proper cellular response to this stress (20). In this regard, first of all, UPR activation upon G14 treatment was analyzed in a *S. saccharomyces* strain with GFP-tagged IRE1, ATF6, and PERK genes. Increased expression of the protein complex was observed by fluorescence microscopy, supporting the prediction that G14 interferes with the N-glycosylation of proteins, activating the UPR. Corroborating these results, real-time PCR analysis of IRE1 and HAC1 genes after G14 treatment revealed the activation of the UPR by the upregulation of these genes.

If the execution of the UPR is unsuccessful, the apoptosis response is induced. This response is deeply linked to mitochondrion activity since there is a physiological and functional interaction between the mitochondrial and ER organelles. This connection is essential to maintain cellular homeostasis and viability (29). The MTT assay confirmed the chronic activation of UPR signaling in which G14 decreases mitochondrial activity and the viability rate of *P. lutzii* cells. The low mitochondrial activity impairs fungal metabolism and the composition and formation of the cell wall. As a consequence, there was interference with bud formation (25, 30), as shown after the G14 treatment of *P. lutzii* cells. The effects of G14 on fungal viability and wall damage were confirmed by CFU enumeration and trypan blue assays. A trypan blue assay confirmed that G14 impairs the fungal cell wall, and CFU enumeration confirmed that a consequence of the weaker fungal cell was a loss of viability.

All of these results confirmed that the fungal wall is important to fungal viability and highlighted how the N-glycosylation process is vital to the integrity of the fungal cell wall. For *Paracoccidioides* spp. the composition of the cell wall is considered an important virulence factor, and its components are important for some properties, such as adhesion to host cells (31).

The dynamics of the interaction of *Paracoccidioides brasiliensis* with human lung epithelial cells (A549) was previously studied by our group (32), and we demonstrated that the interaction rate of the fungi with these cells increases progressively after 3 h of contact, and with 5 h the internalization process was observed. Considering this

knowledge, it was evaluated if the destabilization of the fungal cell wall by G14 treatment *in vitro* influences the interaction with the host cell. For this, A549 cells were challenged with *P. lutzii* for 6 h, ensuring that the cells were adhered and internalized. From this point, the interaction was treated with G14 for 24 h. In comparison with the rate for the control, we observed a significant reduction in the interaction rate, and after applying the quenching test, it was possible to conclude that this reduction was in the adhesion rate since no differences in rates of internalization of fungi were observed. The action of G14 in reducing the adhesion rate could be explained by the destabilization this compound caused to the *P. lutzii* cell wall, as shown in this study. Although the numbers of CFU of the internalized fungal cells were not different between the untreated control and the treated cells, the prevention of fungal adherence to host cells could be an important tool to avoid fungal colonization at different sites, helping to avoid a systemic infection.

Since G14 was able to decrease the *Paracoccidioides* sp. infection, hindering proper fungal adhesion to host cells, we verified whether G14 could help the host control *Paracoccidioides* infection. *Paracoccidioides* spp. are able to induce the modulation of a chronic inflammatory response via the nitric oxide pathway and to exert a negative modulatory effect on granuloma formation in PCM (33, 34). We evaluated the *in vitro* effect of G14 on nitric oxide modulation in RAW 264.7 macrophages infected with *P. lutzii*. G14 treatment significantly reduced nitrite production. We suggest that G14 may play an important role in balancing the inflammatory reaction caused by fungal infection without interfering with the microbicidal activity of nitric oxide. However, when CFU analysis of fungal cells internalized by macrophages was performed, a significant reduction upon treatment was observed, which could mean that G14 treatment had a positive influence on other microbicidal mechanisms of the macrophages.

Antifungal agents acting in the modulation of nitric oxide could be considered excellent candidates for therapy in pathophysiological processes. Lopes et al. (12) demonstrated the anti-inflammatory activity of an alkyl gallate, which has a well-described antioxidant activity and could act as an anti-inflammatory agent and protect human cells against oxidative damage caused by reactive oxygen species. In this way, G14 could also act as an antioxidant compound and be able to reduce the inflammation and damage generated during fungal infection.

In conclusion, through this work we know more about the action of G14, which is involved in the impairment of the N-glycosylation pathway. This effect damages the maintenance of the fungal wall, which results in an important decrease in the infection process *in vitro*, in addition to the important anti-inflammatory role of G14. This study highlights the need for continued studies to promote this compound as a new antifungal agent.

MATERIALS AND METHODS

Decyl gallate (G14). G14 was obtained and provided by Instituto de Química, UNESP (Araraquara, Brazil), according to Morais et al. (35) and prepared according to de Paula e Silva et al. (8).

Chemical-genetic interaction assay. A chemical-genetic interaction assay for G14 was performed as described previously by Piotrowski et al. (36–38) using a *S. cerevisiae* deletion collection pool containing 310 mutants that are functionally representative of all major cellular processes (15, 36). The optimal inhibitory concentration of G14 for a chemical-genetic interaction assay was determined using an eight-point dose-response assay, and a concentration of 7 $\mu\text{g/ml}$ of G14 was determined (70 to 80% growth versus solvent control in yeast extract-peptone [YEP]-galactose medium after 24 h of growth). The deletion collection pool was grown with 7 $\mu\text{g/ml}$ of G14 for 48 h at 30°C. The controls were DMSO, tunicamycin (glycosylation inhibitor), methyl methanesulfonate (MMS; DNA damage inducing agent), micafungin (inhibitor of β -1,3-glucan production of), bortezomib (proteasome inhibitor), and benomyl (microtubule depolymerizing agent), which have known chemical-genetic interaction profiles. After the incubation with G14, the genomic DNA of the deletion collection pool was extracted using an Epicentre MasterPure Yeast DNA purification kit. Special multiplex primers were used to amplify mutant-specific molecular barcodes and to attach unique experiment-specific barcodes to each compound-treated pool (19). Illumina MiSeq was used to sequence the barcodes. The barcode counts for each yeast deletion mutant in the presence of G14 were compared to those under DMSO control conditions to determine sensitivity or resistance of individual strains in the pool (the chemical-genetic interaction score) (15). A Bonferroni-corrected hypergeometric distribution test was used to search for significant enrichment of

GO terms among the top 10 sensitive and resistant deletion mutants (39). Correlation of the chemical-genetic interaction profile of G14 with the yeast genetic interaction network was performed by a bioinformatics program (36, 38).

UPR activation assay. *S. cerevisiae* yeast strain YMJ003 (*ura3Δ::UPRE-GFP-TEF2pr-RFP-MET-URA3 his3Δ1 leu2Δ0 met15Δ0 ura3Δ0 LYS⁺ can1Δ::STE2pr-spHIS5 lyp1Δ::STE3pr-LEU2 CYH2*) was used. This strain has a green fluorescent protein (GFP) tagged to inositol-requiring enzyme 1 (IRE1), activating transcription factor 6 (ATF6), and protein kinase RNA-like endoplasmic reticulum kinase (PERK) genes and was used for UPR analysis (40). A colony was cultivated in 2 ml of synthetic defined medium lacking Trp (SD-Trp) for 18 h at 30°C and 150 rpm. The suspension was diluted 1:10 in SD tryptophan drop-out (SD DO-Trp) medium and incubated for 3 h (log phase) at 30°C and 150 rpm. One milliliter of suspension was diluted in 1 ml of SD DO-Trp medium with 7 μg/ml G14 or in DMSO for 3 and 24 h at 30°C with shaking (150 rpm). At each time point the suspension was centrifuged at 10,000 rpm for 1 min, and the yeast cells were observed by fluorescence microscopy; the mean fluorescence intensity (MFI) was calculated using ImageJ software (NIH).

***P. lutzii* conditions.** The maintenance and the inoculum of *P. lutzii* strain 01 (ATCC MYA-826) were performed according to Scorzoni et al. (41).

Evaluation of N-glycosylation in *P. lutzii*. A suspension of 10⁶ *P. lutzii* cells/ml in brain heart infusion (BHI) broth was treated with a final concentration of 0.5 μg/ml G14 for 3 days at 37°C and 150 rpm. DMSO in the same proportion was used as a control. The fungal suspension was centrifuged at 4,000 rpm at 4°C for 10 min, and the obtained pellet was used in the following experiments.

(i) Enzyme activity measurement of N-glycosylated enzymes. The pellet was washed twice with phosphate-buffered saline (PBS) containing 1 mM phenylmethylsulfonyl fluoride. Cells were disrupted by sonication, followed by centrifugation (10,000 rpm) for 15 min at 4°C for the crude protein extract obtained from the supernatant. Protein concentration was quantified by bicinchoninic acid assay (Pierce Chemical Co.), with bovine serum albumin as the standard (42). Activity of α-(1,4)-amylase (α-amylase) was assayed by monitoring starch hydrolysis (43). One unit of α-(1,4)-amylase activity was described as the amount of enzyme required to hydrolyze 0.1 mg of starch/min. Activity of α-(1,3)-glucanase was determined using α-glucan from *Aspergillus niger* as the substrate (26). One unit of α-(1,3)-glucanase activity was defined as the amount of enzyme required to produce 1 μM reducing sugars/min. *N*-Acetyl-β-D-glucosaminidase (NAGase) activity was verified by monitoring the rate of formation of *p*-nitrophenol from *p*-nitrophenol-β-*N*-acetylglucosamine (pNPGlcNAc; Sigma) (25, 44). One unit of *N*-acetyl-β-D-glucosaminidase activity was defined as the amount of protein required to produce 1 μM *p*-nitrophenol/min at 37°C. The enzyme activity values correspond to the mean values of at least three replicates.

(ii) Evaluation of glycosylated components of fungal cell wall. Fungal suspensions with and without G14 treatment were incubated separately with 100 μg/ml of concanavalin A (ConA), conjugated to Alexa Fluor 488 (Invitrogen), and 100 μg/ml of calcofluor white (CFW; Sigma) at 37°C for 30 min as described by de Curcio et al. (28). The fungal cells were washed, suspended in PBS, and submitted to analysis by a BD FACSCanto I flow cytometer. The mean fluorescence intensity (MFI) of 10,000 cells in the fluorescein isothiocyanate (FITC) channel was calculated. ConA-labeled fungal cells were positive for glycosylated proteins. The CFW-labeled cells were analyzed under a fluorescence microscope. A total of 300 cells (triplicate) were analyzed using ImageJ software (NIH) measuring the MFI of CFW to determine the chitin amount, which is N-glycosylated-enzyme dependent.

(iii) Differential gene expression analysis. RNA from *P. lutzii* with and without G14 treatment was extracted using the TRIzol method (Invitrogen). cDNA synthesis was performed using RevertAid H Minus Reverse Transcriptase (Fermentas) according to the manufacturer's instructions using 1 μg of total RNA. The relative expression levels of the α-(1,3)-glucanase (*agn*), *N*-acetyl-β-D-glucosaminidase (*nag1*), α-(1,4)-amylase (*amy*), inositol requiring enzyme-1 (*ire1*), and transcription factor (*hac1*) genes were analyzed (Table 2). α-Tubulin (*tub*) was used as the housekeeping gene. The reactions were carried out using 1 μl of cDNA, 10 μl of Maximum SYBR green/ROX qPCR Master Mix (2×) (Qiagen), and 0.5 μM each primer. The PCR conditions were as follows: an initial temperature of 95°C for 1 min, followed by 40 cycles of 5 s at 95°C and 60°C for 32 s. The signal emission corresponding to a single product was confirmed by melt curve analysis. Reactions were performed in triplicate with an Applied Biosystems 7500 cyclor (Applied Biosystems). Data were analyzed using the 2^{-ΔΔCT} method (where C_T is threshold cycle) (45).

Influence of G14 on *P. lutzii*. A total of 10⁶ fungal cells/ml in BHI broth were treated with 0.5 μg/ml G14 in a 96-well plate at 37°C in 5% CO₂ for 24 and 48 h. The fungal cell was analyzed by MTT assay, bud formation, trypan blue assay, and CFU enumeration. After the treatment, trypan blue reagent (Sigma) was added to the cells, and the percentage of nonblue cells was measured in a total of 100 cells. Also 100 cells were used to analyze bud formation. For this, cells were separated in two groups: (i) cells with only one or without any buds and (ii) cells with more than one bud. In the CFU enumeration assay, an aliquot of 100 μl was diluted (1:100) in PBS and plated on solid BHI medium supplemented with 4% fetal calf serum, 5% *P. brasiliensis* (strain 192)-spent culture medium, 1.5% glucose, and gentamicin (40 mg/ml) and incubated at 37°C for 15 days, and colonies were counted (46). For the MTT assay, the 96-well plate was centrifuged for 2 min at 5,000 rpm. The supernatant was carefully removed, and 10 μl of MTT solution (5 mg/ml in PBS) plus 40 μl of PBS was added and incubated at 37°C in 5% CO₂ for 4 h. The formazan precipitate was solubilized with 100 μl/well of pure DMSO. The supernatant was transferred to other plate and read by spectrophotometer at 570 nm (690-nm reference).

Influence of G14 on *P. lutzii*-A549 cell interaction. The human lung epithelial cells (A549) were obtained from Banco de Células do Rio de Janeiro (BCRJ). All the cultivation conditions were performed according to BCRJ instructions. A total of 10⁶ cells/ml were plated in a 96-well plate in monolayer

formation at 37°C in 5% CO₂. Cells were challenged with 10⁶ *P. lutzii* cells/ml labeled with 0.5 mg/ml of fluorescein isothiocyanate (FITC; Sigma) for 6 h at 37°C in 5% CO₂. The supernatant was removed, and the infection was washed with PBS and treated with 0.5 µg/ml G14 in Dulbecco's modified Eagle's medium (DMEM) for 24 h at 37°C in 5% CO₂. After the incubation, the interaction was analyzed by flow cytometry and CFU enumeration as described below.

(i) Flow cytometry analysis. The supernatant was carefully removed, and 0.065 µM Alexa Fluor 647-phalloidin (ThermoFisher Scientific) solution prepared in cold 4% paraformaldehyde (Sigma) with 0.5% Triton X-100 (Amersham Biosciences) was added to the cells for 20 min. The cells were recovered in PBS and submitted to analysis by BD FACSCanto I flow cytometer. A total of 10,000 events were acquired from Alexa Fluor 647-positive events (allophycocyanin [APC] filter for the host cell population). FITC-positive events (FITC filter for the fungal cell population) were analyzed from the APC-positive population. This relation reveals the percentage of fungal cells interacting with host cells, termed the interaction rate. To the remaining suspension, 200 µg/ml trypan blue (Sigma) was added and incubated for 10 min at room temperature to quench FITC fluorescence of externally adhered fungal cells. Trypan blue reagent is able to decrease the fluorescence intensity of FITC, and it is not capable of reaching the intracellular host compartment, thus differentiating intracellular and adhered fungal cells (47). A total of 10,000 events were acquired from APC-positive events gate, obtaining a rate of fungal cells (FITC positive) internalized in the host cells. For the estimation of adhered cells, the internalized fungal cell rate was subtracted from interaction rate.

(ii) CFU enumeration. The supernatant was discarded, and the nonadherent fungal cells were removed with PBS washes. Subsequently, 15 µg/ml of ketoconazole (Sigma) in DMEM was added for 1 h at 37°C to kill only the adhered fungi, followed by PBS washes to remove them. The A549 cells were lysed with 100 µl of sterile MilliQ water (32), and the suspension was plated on solid BHI medium supplemented as described previously and incubated at 37°C for 15 days for colony counts (46). The CFU count obtained indicates fungal cells that were internalized.

Anti-*P. lutzii* activity of macrophage due to G14 modulation. RAW 264.7 macrophages were obtained from BCRJ, and all the cultivation conditions were performed according to BCRJ instructions. The macrophage suspension was adjusted to 10⁶ cells/ml, and 100 µl was plated in a 96-well plate in monolayer formation at 37°C in 5% CO₂. After macrophage monolayer formation, the supernatant was carefully removed, and cells were infected with 100 µl at 10⁶ *P. lutzii* cells/ml in DMEM or treated with 0.2 mg/ml lipopolysaccharide (LPS) in DMEM (positive control) or only DMEM (negative control). The plates were incubated at 37°C in 5% CO₂ for 6 h. After this the supernatant was removed, and the monolayer was carefully washed with PBS and treated with 0.5 µg/ml G14 for 24 h at 37°C in 5% CO₂. Nitrite production was evaluated using a Griess assay (12, 48). For this, the supernatants were transferred to another plate and mixed 1:1 with 100 µl/well fresh solution of *N*-(1-naphthyl) ethylenediamine dihydrochloride (NEED; 0.1%) and sulfanilamide (1%, vol/vol). The reaction was read by spectrophotometer at 540 nm. The viability of *P. lutzii* cells internalized by macrophages was determined by CFU analysis. This assay was conducted as described above.

Statistical analyses. Graphs and statistical analyzes were performed with GraphPad Prism, version 5 (La Jolla, CA, USA), using a *t* test.

ACKNOWLEDGMENTS

This work was supported by Rede Nacional de Métodos Alternativos, Conselho Nacional de Pesquisa e Desenvolvimento (RENAMA-CNPq) (403586/2012-7), Fundação de Amparo à Pesquisa do Estado de São Paulo (FAPESP) (2016/17048-4 to C.M.M., 2015/03700-9 to M.J.S.M.-G., 2015/14023-8 to H.C.D.O., and 2013/10917-9 to L.S.), Coordenação de Aperfeiçoamento de Pessoal de Nível Superior (CAPES), Programa de Doutorado Sanduíche no Exterior (PDSE), Programa de Apoio ao Desenvolvimento Científico da Faculdade de Ciências Farmacêuticas da UNESP (PADC/FCF), and Pró-Reitora de Pesquisa da UNESP (PROPe/UNESP).

REFERENCES

- Shikanai-Yasuda MA, Mendes RP, Colombo AL, Queiroz-Telles F, Kono ASG, Paniago AMM, Nathan A, Valle A, Bagagli E, Benard G, Ferreira MS, Teixeira MM, Silva-Vergara ML, Pereira RM, Cavalcante RS, Hahn R, Durlacher RR, Khoury Z, Camargo ZP, Moretti ML, Martinez R. 2017. Brazilian guidelines for the clinical management of paracoccidioidomycosis. *Rev Soc Bras Med Trop* 50:715–740. <https://doi.org/10.1590/0037-8682-0230-2017>.
- Martinez R. 2015. Epidemiology of paracoccidioidomycosis. *Rev Inst Med Trop S Paulo* 57(Suppl 19):11–20. <https://doi.org/10.1590/S0036-46652015000700004>.
- San-Blas G, Urbina JA, Marchan E, Contreras LM, Sorais F, San-Blas F. 1997. Inhibition of *Paracoccidioides brasiliensis* by ajoene is associated with blockade of phosphatidylcholine biosynthesis. *Microbiology* 143: 1583–1586. <https://doi.org/10.1099/00221287-143-5-1583>.
- Thomaz L, Apitz-Castro R, Marques AF, Travassos LR, Taborda CP. 2008. Experimental paracoccidioidomycosis: alternative therapy with ajoene, compound from *Allium sativum*, associated with sulfamethoxazole/trimethoprim. *Med Mycol* 46:113–118. <https://doi.org/10.1080/13693780701651681>.
- Martins CVB, da Silva DL, Neres ATM, Magalhães TFF, Watanabe GA, Modolo LV, Sabino AA, de Fátima A, de Resende MA. 2009. Curcumin as a promising antifungal of clinical interest. *J Antimicrob Chemother* 63:337–339. <https://doi.org/10.1093/jac/dkn488>.
- de Sá NP, Cisalpino PS, Tavares LC, Espindola L, Pizzolatti MG, Santos PC, de Paula TP, Rosa CA, de Souza DG, Santos DA, Johann S. 2015. Antifungal activity of 6-quinolinyl *N*-oxide chalcones against *Paracoccidioides*. *J Antimicrob Chemother* 70:841–845. <https://doi.org/10.1093/jac/dku427>.
- Johann S, Cisalpino PS, Watanabe GA, Cota BB, de Siqueira EP, Pizzolatti MG, Zani CL, de Resende MA. 2010. Antifungal activity of extracts of

- some plants used in Brazilian traditional medicine against the pathogenic fungus *Paracoccidioides brasiliensis*. *Pharm Biol* 48:388–396. <https://doi.org/10.3109/13880200903150385>.
8. de Paula e Silva ACA, Costa-Orlandi CB, Gullo FP, Sangalli-Leite F, de Oliveira HC, Silva J. d F d, Scorzoni L, Pitangui N. d S, Rossi SA, Benaducci T, Wolf VG, Regasini LO, Petrônio MS, Silva DHS, Bolzani VS, Fusco-Almeida AM, Mendes-Giannini MJS. 2014. Antifungal activity of decyl gallate against several species of pathogenic fungi. *Evid Based Complement Alternat Med* 2014:506273. <https://doi.org/10.1155/2014/506273>.
 9. Gullo FP, Sardi JC, Santos VA, Sangalli-Leite F, Pitangui NS, Rossi SA, de Paula E Silva AC, Soares LA, Silva JF, Oliveira HC, Furlan M, Silva DH, Bolzani VS, Mendes-Giannini MJ, Fusco-Almeida AM. 2012. Antifungal activity of maytenin and pristimerin. *Evid Based Complement Alternat Med* 2012:340787. <https://doi.org/10.1155/2012/340787>.
 10. Calvo TR, Lima ZP, Silva JS, Ballesteros KV, Pellizzon CH, Hiruma-Lima CA, Tamashiro J, Brito AR, Takahira RK, Vilegas W. 2007. Constituents and antiulcer effect of *Alchornea glandulosa*: activation of cell proliferation in gastric mucosa during the healing process. *Biol Pharm Bull* 30: 451–459. <https://doi.org/10.1248/bpb.30.451>.
 11. Treviño-Cueto B, Luis M, Contreras-Esquivel JC, Rodríguez R, Aguilera A, Aguilar CN. 2007. Gallic acid and tannase accumulation during fungal solid state culture of a tannin-rich desert plant (*Larrea tridentata* Cov.). *Bioresour Technol* 98:721–724. <https://doi.org/10.1016/j.biortech.2006.02.015>.
 12. Lopes FC, Calvo TR, Vilegas W, Carlos IZ. 2005. Inhibition of hydrogen peroxide, nitric oxide and TNF- α production in peritoneal macrophages by ethyl acetate fraction from *Alchornea glandulosa*. *Biol Pharm Bull* 28:1726–1730. <https://doi.org/10.1248/bpb.28.1726>.
 13. Lopes FC, Rocha A, Pirraco A, Regasini LO, Siqueira JR, Silva DH, Bolzani VS, Carlos IZ, Soares R. 2011. *Alchornea glandulosa* ethyl acetate fraction exhibits antiangiogenic activity: preliminary findings from in vitro assays using human umbilical vein endothelial cells. *J Med Food* 14:1244–1253. <https://doi.org/10.1089/jmf.2010.0204>.
 14. Leal PC, Mascarello A, Derita M, Zuljan F, Nunes RJ, Zacchino S, Yunes RA. 2009. Relation between lipophilicity of alkyl gallates and antifungal activity against yeasts and filamentous fungi. *Bioorg Med Chem Lett* 19:1793–1796. <https://doi.org/10.1016/j.bmcl.2009.01.061>.
 15. Parsons AB, Lopez A, Givoni IE, Williams DE, Gray CA, Porter J, Chua G, Sopko R, Brost RL, Ho CH, Wang J, Ketela T, Brenner C, Brill JA, Fernandez GE, Lorenz TC, Payne GS, Ishihara S, Ohya Y, Andrews B, Hughes TR, Frey BJ, Graham TR, Andersen RJ, Boone C. 2006. Exploring the mode-of-action of bioactive compounds by chemical-genetic profiling in yeast. *Cell* 126:611–625. <https://doi.org/10.1016/j.cell.2006.06.040>.
 16. Ho CH, Piotrowski J, Dixon SJ, Baryshnikova A, Costanzo M, Boone C. 2011. Combining functional genomics and chemical biology to identify targets of bioactive compounds. *Curr Opin Chem Biol* 15:66–78. <https://doi.org/10.1016/j.cbpa.2010.10.023>.
 17. Fung SY, Sofyev V, Schneiderman J, Hirschfeld AF, Victor RE, Woods K, Piotrowski JS, Deshpande R, Li SC, de Voogd NJ, Myers CL, Boone C, Andersen RJ, Turvey SE. 2014. Unbiased screening of marine sponge extracts for anti-inflammatory agents combined with chemical genomics identifies girolline as an inhibitor of protein synthesis. *ACS Chem Biol* 9:247–257. <https://doi.org/10.1021/cb400740c>.
 18. Williams DE, Dalisay DS, Patrick BO, Maitainaho T, Andrusiak K, Deshpande R, Myers CL, Piotrowski JS, Boone C, Yoshida M, Andersen RJ. 2011. Padanamides A and B, highly modified linear tetrapeptides produced in culture by a *Streptomyces* sp. isolated from a marine sediment. *Org Lett* 13:3936–3939. <https://doi.org/10.1021/ol2014494>.
 19. Smith AM, Heisler LE, Mellor J, Kaper F, Thompson MJ, Chee M, Roth FP, Giaever G, Nislow C. 2009. Quantitative phenotyping via deep barcode sequencing. *Genome Res* 19:1836–1842. <https://doi.org/10.1101/gr.093955.109>.
 20. Krishnan K, Askew DS. 2014. Endoplasmic reticulum stress and fungal pathogenesis. *Fungal Biol Rev* 28:29–35. <https://doi.org/10.1016/j.fbr.2014.07.001>.
 21. Elbein AD. 1987. Inhibitors of the biosynthesis and processing of N-linked oligosaccharide chains. *Annu Rev Biochem* 56:497–534. <https://doi.org/10.1146/annurev.bi.56.070187.002433>.
 22. Jakob CA, Burda P, Roth J, Aebi M. 1998. Degradation of misfolded endoplasmic reticulum glycoproteins in *Saccharomyces cerevisiae* is determined by a specific oligosaccharide structure. *J Cell Biol* 142: 1223–1233. <https://doi.org/10.1083/jcb.142.5.1223>.
 23. Lodish H, Berk A, Zipursky SL. 2000. Protein glycosylation in the ER and Golgi complex, section 17.7. In Lodish H, Berk A, Zipursky SL, Matsudaira P, Baltimore D, Darnell J (ed), *Molecular cell biology*, 4th ed. W. H. Freeman, New York, NY.
 24. Free SJ. 2013. Fungal cell wall organization and biosynthesis. *Adv Genet* 81:33–82. <https://doi.org/10.1016/B978-0-12-407677-8.00002-6>.
 25. Dos Reis Almeida FB, Carvalho FC, Mariano VS, Alegre ACP, Silva R. d N, Hanna ES, Roque-Barreira MC. 2011. Influence of N-glycosylation on the morphogenesis and growth of *Paracoccidioides brasiliensis* and on the biological activities of yeast proteins. *PLoS One* 6:e29216. <https://doi.org/10.1371/journal.pone.0029216>.
 26. Dos Reis Almeida FB, Pigosso LL, de Lima Damasio AR, Monteiro VN, de Almeida Soares CM, Silva RN, Roque-Barreira MC. 2014. α -(1,4)-Amylase, but not α - and β -(1,3)-glucanases, may be responsible for the impaired growth and morphogenesis of *Paracoccidioides brasiliensis* induced by N-glycosylation inhibition. *Yeast* 31:1–11. <https://doi.org/10.1002/yea.2983>.
 27. Almeida F, Antonieto AC, Pessonni AM, Monteiro VN, Alegre-Maller AC, Pigosso LL, Pereira M, Soares CM, Roque-Barreira MC. 2016. Influence of N-glycans on expression of cell wall remodeling related genes in *Paracoccidioides brasiliensis* yeast cells. *Curr Genomics* 17:112–118. <https://doi.org/10.2174/1389202917666151116212705>.
 28. de Curcio JS, Silva MG, Silva Bailão MG, Bão SN, Casaletti L, Bailão AM, de Almeida Soares CM. 2017. Identification of membrane proteome of. *Future Sci OA* 3:FSO232. <https://doi.org/10.4155/fsoa-2017-0044>.
 29. Malhotra JD, Kaufman RJ. 2011. ER stress and its functional link to mitochondria: role in cell survival and death. *Cold Spring Harb Perspect Biol* 3:a004424. <https://doi.org/10.1101/cshperspect.a004424>.
 30. Carbonell LM. 1967. Cell wall changes during the budding process of *Paracoccidioides brasiliensis* and *Blastomyces dermatitidis*. *J Bacteriol* 94:213–223.
 31. Camacho E, Nino-Vega GA. 2017. *Paracoccidioides* spp.: virulence factors and immune-evasion strategies. *Mediators Inflamm* 2017:5313691. <https://doi.org/10.1155/2017/5313691>.
 32. Mendes-Giannini MJ, Hanna SA, da Silva JL, Andreotti PF, Vincenzi LR, Benard G, Lenzi HL, Soares CP. 2004. Invasion of epithelial mammalian cells by *Paracoccidioides brasiliensis* leads to cytoskeletal rearrangement and apoptosis of the host cell. *Microbes Infect* 6:882–891. <https://doi.org/10.1016/j.micinf.2004.05.005>.
 33. Nishikaku AS, Molina RF, Ribeiro LC, Scavone R, Albe BP, Cunha CS, Burger E. 2009. Nitric oxide participation in granulomatous response induced by *Paracoccidioides brasiliensis* infection in mice. *Med Microbiol Immunol* 198:123–135. <https://doi.org/10.1007/s00430-009-0113-x>.
 34. Burger E, Nishikaku AS, Gameiro J, Francelin C, Camargo ZP, Verinaud L. 2013. Cytokines expressed in the granulomatous lesions in experimental paracoccidioidomycosis: role in host protective immunity and as fungal virulence factor. *J Clin Cell Immunol* S1:010. <https://doi.org/10.4172/2155-9899.S1-010>.
 35. Morais MC, Luqman S, Kondratyuk TP, Petronio MS, Regasini LO, Silva DH, Bolzani VS, Soares CP, Pezzuto JM. 2010. Suppression of TNF- α induced NF- κ B activity by gallic acid and its semi-synthetic esters: possible role in cancer chemoprevention. *Nat Prod Res* 24:1758–1765. <https://doi.org/10.1080/14786410903335232>.
 36. Piotrowski JS, Li SC, Deshpande R, Simpkins SW, Nelson J, Yashiroda Y, Barber JM, Safizadeh H, Wilson E, Okada H, Gebre AA, Kubo K, Torres NP, LeBlanc MA, Andrusiak K, Okamoto R, Yoshimura M, DeRango-Adem E, van Leeuwen J, Shirahige K, Baryshnikova A, Brown GW, Hirano H, Costanzo M, Andrews B, Ohya Y, Osada H, Yoshida M, Myers CL, Boone C. 2017. Functional annotation of chemical libraries across diverse biological processes. *Nat Chem Biol* 13:982–993. <https://doi.org/10.1038/nchembio.2436>.
 37. Piotrowski JS, Okada H, Lu F, Li SC, Hinchman L, Ranjan A, Smith DL, Higbee AJ, Ulbrich A, Coon JJ, Deshpande R, Bukhman YV, McIlwain S, Ong IM, Myers CL, Boone C, Landick R, Ralph J, Kabbage M, Ohya Y. 2015. Plant-derived antifungal agent poaic acid targets beta-1,3-glucan. *Proc Natl Acad Sci U S A* 112:E1490–E1497. <https://doi.org/10.1073/pnas.1410400112>.
 38. Piotrowski JS, Simpkins SW, Li SC, Deshpande R, McIlwain SJ, Ong IM, Myers CL, Boone C, Andersen RJ. 2015. Chemical genomic profiling via barcode sequencing to predict compound mode of action. *Methods Mol Biol* 1263:299–318. https://doi.org/10.1007/978-1-4939-2269-7_23.
 39. Boyle EI, Weng S, Gollub J, Jin H, Botstein D, Cherry JM, Sherlock G. 2004. GO:TermFinder—open source software for accessing Gene Ontology information and finding significantly enriched Gene Ontology terms associated with a list of genes. *Bioinformatics* 20:3710–3715. <https://doi.org/10.1093/bioinformatics/bth456>.

40. Jonikas MC, Collins SR, Denic V, Oh E, Quan EM, Schmid V, Weibezahn J, Schwappach B, Walter P, Weissman JS, Schuldiner M. 2009. Comprehensive characterization of genes required for protein folding in the endoplasmic reticulum. *Science* 323:1693–1697. <https://doi.org/10.1126/science.1167983>.
41. Scorzoni L, de Paula e Silva AC, Singulani JL, Leite FS, de Oliveira HC, da Silva RA, Fusco-Almeida AM, Mendes-Giannini MJ. 2015. Comparison of virulence between *Paracoccidioides brasiliensis* and *Paracoccidioides lutzii* using *Galleria mellonella* as a host model. *Virulence* 6:766–776. <https://doi.org/10.1080/21505594.2015.1085277>.
42. dos Reis Almeida FB, de Oliveira LL, Valle de Sousa M, Roque Barreira MC, Hanna ES. 2010. Paracoccin from *Paracoccidioides brasiliensis*; purification through affinity with chitin and identification of N-acetyl-beta-D-glucosaminidase activity. *Yeast* 27:67–76. <https://doi.org/10.1002/yea.1731>.
43. Fuwa H. 1954. A new method for microdetermination of amylase activity by the use of amylose as the substrate. *J Biochem* 4:583–603. <https://doi.org/10.1093/oxfordjournals.jbchem.a126476>.
44. Almeida F, Sardinha-Silva A, da Silva TA, Pessoni AM, Pinzan CF, Alegremaller ACP, Cecílio NT, Moretti NS, Damásio ARL, Pedersoli WR, Mineo JR, Silva RN, Roque-Barreira MC. 2015. *Toxoplasma gondii* Chitinase induces macrophage activation. *PLoS One* 10:e0144507. <https://doi.org/10.1371/journal.pone.0144507>.
45. Livak KJ, Schmittgen TD. 2001. Analysis of relative gene expression data using real-time quantitative PCR and the $2^{-\Delta\Delta CT}$ method. *Methods* 25:402–408. <https://doi.org/10.1006/meth.2001.1262>.
46. Singulani JL, Scorzoni L, Lourencetti NMS, Oliveira LR, Conçolaro RS, da Silva PB, Nazaré AC, Polaquini CR, Victorelli FD, Chorilli M, Regasini LO, Fusco Almeida AM, Mendes Giannini M. 2018. Potential of the association of dodecyl gallate with nanostructured lipid system as a treatment for paracoccidioidomycosis: in vitro and in vivo efficacy and toxicity. *Int J Pharm* 547:630–636. <https://doi.org/10.1016/j.ijpharm.2018.06.013>.
47. Nogueira SV, Fonseca FL, Rodrigues ML, Mundodi V, Abi-Chacra EA, Winters MS, Alderete JF, de Almeida Soares CM. 2010. *Paracoccidioides brasiliensis* enolase is a surface protein that binds plasminogen and mediates interaction of yeast forms with host cells. *Infect Immun* 78:4040–4050. <https://doi.org/10.1128/IAI.00221-10>.
48. Salina AC, Souza TP, Serezani CH, Medeiros AI. 2017. Efferocytosis-induced prostaglandin E2 production impairs alveolar macrophage effector functions during *Streptococcus pneumoniae* infection. *Innate Immun* 23:219–227. <https://doi.org/10.1177/1753425916684934>.